Susceptibilities and Critical Fields of Superconducting Films*

WERNER LINIGER AND FAROUK ODEH
Thomas J. Watson Research Center, International Business Machines Corporation, Yorktown Heights, New York

(Received 17 July 1963)

The present report concerns the calculation of field distributions, susceptibilities, and critical fields of a superconducting film using the nonlocal and nonlinear (Ginzburg–Landau) theories with diffuse scattering boundary conditions. Both the Pippard and the BCS kernels are considered. The main tool in obtaining these results is a numerical calculation of the vector potential, but an analytical treatment is possible in the very thin film and bulk limits. A comparison between the results obtained with the two different kernels is made for field distributions and susceptibilities. The present susceptibilities are compared with those for diffuse scattering calculated by Rogers and Schrieffer and with Toxen's results for specular reflection. Maximum fields are obtained from a nonlinear-nonlocal generalization of the Ginzburg–Landau equations due to Bardeen. These equations are solved by a mixture of perturbation and numerical methods using the Pippard kernel. The dependence of these maximum fields on the coherence length is studied, and the present results are compared with Toxen's critical fields for specular reflection. In the thin film limit, the present calculation establishes on a rigorous basis the proportionality of the critical field to the negative three-halves power of thickness. It is shown that there exist two types of transition and a critical thickness in the nonlocal-nonlinear case, just as in the Ginzburg–Landau theory. The type of transition changes, for fixed thickness, from first to second order when the coherence length is raised beyond a certain value.

INTRODUCTION

NUMEROUS experimental and theoretical investigations[1,2] of the electromagnetic behavior of superconductors have indicated that London's phenomenological model should be generalized in two directions. First, a nonlocal theory is needed to account for mean free path, impurity contents, and similar effects. Second, a field-dependent description of the properties of a superconductor, i.e., a nonlinear theory, is needed to account for strong field effects. The phenomenological model of Pippard, which is similar to the results of the Bardeen-Cooper-Schrieffer (BCS) microscopic theory, together with the Ginzburg-Landau (GL) theory seem to adequately generalize London's model. Several calculations of important properties of superconducting films have been carried out on the basis of either of the above mentioned theories. Schrieffer[3] calculated susceptibilities of such films in the two cases of specular and diffuse scattering at the surface and derived an analytical solution for the specular reflection case. Sommerhalder and Thomas[4,5] discussed the problem of the sign reversal of a magnetic field penetrating a superconductor. In order to estimate the critical fields of superconducting films, Toxen[6] used a model in which he equated Schrieffer's susceptibility to the one derived from the GL theory. A similar procedure was employed by Hauser and Helfand.[7] In the case of diffuse scattering, no calculations of critical fields seem to have been done except for very thin films.[6] This may be due to the fact that no closed-form solutions to the nonlocal equations with these boundary conditions exist at present. Even in the case of susceptibilities, much less attention has been paid to the diffuse scattering case, for the same reason. Aside from a result of Rogers[8] for the thin film limit, the only one the authors know of is Schrieffer's result which was obtained by a variational method retaining only a few terms in the trial solution. Also, only the Pippard kernel was considered.

This report is concerned mainly with obtaining both the susceptibilities and maximum fields[9] of plane films from a direct numerical integration of the relevant integral-differential equations. *The diffuse scattering boundary conditions will be the only ones used.* For convenience, the plan of the paper is outlined at this point: In Sec. 1, the methods for calculating field distributions, both with the Pippard and the BCS kernels (at zero temperature) are described. Sec. 2 consists of two parts. In the first, susceptibilities are obtained for both kernels from the numerical field distributions. A separate analytical treatment is employed for the limiting case of very thin films. In the second part, maximum fields are obtained from a generalization of the GL equations, due to Bardeen,[1] which includes both nonlocal and nonlinear effects. These equations are solved by a mixture of perturbation and numerical methods. Only the Pippard kernel has been considered. A special analytical treatment is used to calculate the fields

* An abstract of the present paper was published in Phys. Rev. Letters **10**, 47 (1963).
[1] J. Bardeen, *Encyclopedia of Physics* (Springer-Verlag, Berlin, 1956), Vol. XV, p. 274.
[2] R. Sommerhalder and K. Drangeid, Phys. Rev. Letters **8**, 467 (1962).
[3] J. R. Schrieffer, Phys. Rev. **106**, 47 (1957).
[4] R. Sommerhalder and H. Thomas, Helv. Phys. Acta **34**, 29 (1961).
[5] R. Sommerhalder and H. Thomas, Helv. Phys. Acta **34**, 265 (1961).
[6] A. M. Toxen, Phys. Rev. **127**, 382 (1962).
[7] J. J. Hauser and E. Helfand, Phys. Rev. **127**, 386 (1962).
[8] K. T. Rogers, Ph.D. thesis, University of Illinois, 1960 (unpublished).
[9] See Sec. 2 for explanation of maximum fields.

associated with small values of the order parameter. For the sake of comparison, a critical field calculation similar to that of London, but using nonlocal relations, is included.

In Sec. 3, The results of the present investigation are discussed in detail. A comparison is given between the susceptibilities calculated according to Sec. 2 and previous results of Schrieffer,[3] Toxen,[6] and Rogers.[8] Another comparison between the Pippard and the Bardeen cases shows that the Pippard kernel gives lower susceptibilities for thin films while the converse is true for thicker ones. Also, field distributions with both kernels are considered for various thicknesses, coherence lengths, and penetration depths.

The results deduced from Bardeen's nonlocal-nonlinear equations show the existence of two types of transitions in the nonlocal case, just as in the case of the Ginzburg-Landau equations.[10] The "critical thickness" at which the type of transition changes increases monotonically with the coherence length. Thus, the type of transition in a film can be changed, from first to second order, by raising the coherence length. The maximum field, as a function of thickness, has been plotted for certain values of penetration depth and coherence length. The present maximum fields are higher, but agree qualitatively with Toxen's critical fields obtained from a different model and specular reflection boundary conditions.[6] In the thin film limit, the present result is equivalent to Toxen's result for random scattering and establishes rigorously the proportionality of the critical field to the negative three-halves power of thickness.

1. BASIC EQUATIONS AND NUMERICAL METHODS

A. Pippard Kernel

A numerical solution of the integral-differential equation of the nonlocal theory of superconductivity with diffuse scattering boundary conditions has been carried out by Sommerhalder and Thomas[5] (henceforth referred to as ST) for the case of a hollow cylinder using the Pippard kernel. Their numerical method with appropriate modifications has been used in the present investigation to calculate field distributions across an infinite plane film. In this case, however, the fields applied on the two sides, H_1 and H_2 are independent and relations (2.8) and (2.13) of ST do not apply. Only the symmetrical problem, $H_1=H_2=H_e$, is discussed in the following although some calculations have been done for $H_1\neq H_2$ as well.

Because of the singularity of the kernel, it is useful to integrate by parts in the above-mentioned equation before applying finite difference techniques. In doing so, the auxiliary functions $y(x)=\int_0^x k(t)dt=-y(-x)$ and $z(x)=\int_0^x y(t)dt=z(-x)$, $(x\geq 0)$, are introduced, where $k(t)$ is the Pippard kernel taken in dimensionless form. The functions $y(x)$ and $z(x)$ can be expressed in terms of $E(x)=-e^x\,\mathrm{Ei}(-x)$, where $\mathrm{Ei}(-x)$ is the exponential integral function.[11]

B. BCS Kernel

In BCS theory, the kernel of the basic integral-differential equation for the vector potential is, at zero temperature, defined by Eqs. (5.2) and (C16) of Bardeen, Cooper, and Schrieffer.[12] If these equations are integrated over the coordinates of a plane parallel to the surfaces of the film and the dimensionless variables of ST are used, the BCS kernel takes the form

$$k^*(t)=\int_1^\infty\left(\frac{1}{u}-\frac{1}{u^3}\right)I(tu)du\,, \tag{1.1}$$

$$I(r)=\frac{2}{\pi}\int_{2r/\pi}^\infty K_0(v)dv\,, \tag{1.2}$$

where $K_0(v)$ is the modified Bessel function[13] which decays exponentially for $v\to\infty$. The asterisk is used to distinguish the BCS kernel from the Pippard kernel, $k(t)$, and, by definition, $I(r)=J(\xi_0 r)$.

As in the Pippard case, an integration by parts is carried out in the basic equation, and the same numerical technique is used for solving the resulting modified equation except that the integral is expressed by a quadrature formula and $z^*(x)$ [analogous to $z(x)$] is not used. The function $y^*(x)=\int_0^x k^*(t)dt$ may be calculated numerically as follows. One introduces

$$\phi(u)=\int_0^u I(r)dr\,, \tag{1.3}$$

and finds

$$y^*(s)=\int_1^\infty(t^{-2}-t^{-4})\phi(st)dt\,. \tag{1.4}$$

As stated in Bardeen, Cooper, and Schrieffer,[12] one has

$$I(0)=\int_0^\infty I(r)dr=\phi(\infty)=1\,. \tag{1.5}$$

Thus, (1.2) can be replaced by

$$I(r)=1-\frac{2}{\pi}\int_0^{2r/\pi}K_0(v)dv\,. \tag{1.6}$$

[10] P. M. Marcus, in *Proceedings of the Eighth International Conference on Low Temperature Physics* (Butterworth's Scientific Publications Ltd., London, 1962).

[11] Eugene Jahnke and Fritz Emde, *Tables of Functions* (Dover Publications, Inc., New York, 1945), 4th ed., p. 6.

[12] J. Bardeen, L. N. Cooper, and J. R. Schrieffer, Phys. Rev. **108**, 1175 (1957).

[13] A. Erdelyi, W. Magnus, F. Oberhettinger, and F. G. Tricomi, *Higher Transcendental Functions* (McGraw-Hill Book Company, Inc., New York, 1953), Vol. 2, pp. 5, 19.

For small v, $K_0(v)\approx-[\gamma+\ln(\frac{1}{2}v)]$, where $\gamma=0.577216$ is the Euler constant.[14] Thus, for small r and u,

$$I(r)\approx 1-(4r/\pi^2)[(1-\gamma)+\ln(\pi/r)], \tag{1.7}$$

$$\phi(u)\approx u-(1/\pi^2)[(3-2\gamma+2\ln\pi)-2\ln u]u^2, \tag{1.8}$$

respectively. In evaluating (1.4), one can, according to (1.5), replace $\phi(u)$ by unity for $u\geq\delta\times s$, with a given $s>0$ and sufficiently large δ. The error committed by this replacement can be estimated by using the asymptotic expansion of $\phi(u)$ as $u\to\infty$. Then, (1.4) can be replaced by

$$y^*(s)\approx\int_1^\delta (t^{-2}-t^{-4})\phi(st)dt+\frac{1}{\delta}-\frac{1}{3\delta^3}. \tag{1.9}$$

In order to solve the integral equation, with $y^*(s)$ as a kernel, numerically on a grid $\{s_i=il_1,\ i=0,\ 1,\ \cdots,\ n;\ l_1=\Delta/n\}$, one needs approximate values $y_i^*\approx y^*(s_i)$. To obtain these, the integral in (1.9) is expressed by the trapezoidal rule on a grid $\{t_j=jl_2,\ j=m,\ m+1,\ \cdots;\ l_2=1/m,\ m \text{ integer}\}$. This requires knowing $\phi_\nu\approx\phi(u_\nu)$ on a grid $\{u_\nu=\nu l_3,\ \nu=m,\ m+1,\ \cdots;\ l_3=l_1l_2\}$. Assume $\delta=\zeta l_3$, ζ integer. Then, (1.9) takes the form

$$y_i^*=l_2\Big[\sum_{j=m+1}^{\zeta-1}(t_j^{-2}-t_j^{-4})\phi_{i\times j}+\tfrac{1}{2}(t_\zeta^{-2}-t_\zeta^{-4})\phi_{i\times\zeta}\Big]+\left(\frac{1}{\delta}-\frac{1}{3\delta^3}\right), \tag{1.10}$$

noticing that the integrand vanishes for $j=m$. In (1.10) one has to replace $\phi_{i\times j}$ by unity whenever $i\times j>\zeta$. Thus, ϕ_ν is needed for $m\leq\nu\leq\zeta$.

It will be assumed that l_1 is chosen sufficiently small for (1.7) and (1.8) to apply to the calculation of $I(l_1)$ and $\phi(l_1)$, respectively. Then, the integral in (1.6) can be replaced by one taken from $2l_1/\pi$ to $2r/\pi$, and the integral in (1.3) by one from l_1 to u. If the trapezoidal rule is applied to the former on a grid $\{v_\nu=2\nu l_3/\pi,\ \nu=m,\ m+1,\ \cdots,\ \zeta\}$, it yields I_ν on $\{r_\nu=\nu l_3\}$, and if the same rule is applied to the I_ν, One obtains ϕ_ν on the latter grid, as required above.

2. SUSCEPTIBILITIES AND CRITICAL FIELDS

A. Susceptibilities

Consider a superconducting plane film, defined by $0\leq x\leq D$, in a parallel uniform magnetic field, H_e. In the notations of ST, the susceptibility is given by[3]

$$\kappa/\kappa_0=1-(2/\Delta)F(\Delta), \tag{2.1}$$

where κ_0 is the bulk susceptibility, $F(\Delta)$ the normalized vector potential satisfying the basic integral-differential equation mentioned above and boundary conditions $F'(0)=F'(\Delta)=1$, $\Delta=D/\xi$, and ξ is the effective coherence length. Equation (2.1) has been used, together with the numerical solution, to determine κ/κ_0. For very thin films, however, an analytical approximation is possible and yields more accurate results. The procedure may be sketched as follows.

One introduces the variables $t=s/\Delta$, $t'=s'/\Delta$ and defines $R(t)\cdot\Delta=F(s)$. Then, one has

$$\kappa/\kappa_0=1-2R(1), \tag{2.2}$$

where $R(t)$ satisfies

$$\frac{d^2R}{dt^2}=\alpha\Delta^3\int_0^1 k[\Delta(t-t')]R(t')dt',$$

$$\left.\frac{dR}{dt}\right|_{0,1}=1 \tag{2.3}$$

and $\alpha=3\xi^3/4\xi_0\lambda_0^2$, ξ_0 is the coherence length in pure material, and λ_0 the weak-field penetration depth. By converting (2.3) into a pure integral equation, it becomes amenable to solution by iteration. Let $R(t)=(t-\frac{1}{2})+P(t)$. Then, P satisfies

$$P''(t)=\alpha\Delta^3\left[f(t)+\int_0^1 k[\Delta(t-t')]P(t')dt'\right], \tag{2.4a}$$

$$f(t)=\int_0^1 k[\Delta(t-t')][t'-\tfrac{1}{2}]dt', \tag{2.4b}$$

and

$$\left.\frac{dP}{dt}\right|_{0,1}=0. \tag{2.4c}$$

By use of the generalized Green's function,[15] Eq. (2.4a) can be replaced by the equivalent relation

$$P(t)=\alpha\Delta^3P_0(t)+\alpha\Delta^3\int_0^1 k^{(1)}(t,t')P(t')dt', \tag{2.5a}$$

where

$$P_0(t)=\int_0^1 g(t,t')f(t')dt', \tag{2.5b}$$

$$k^{(1)}(t,t')=\int_0^1 g(t,\xi)k[\Delta(\xi-t')]d\xi, \tag{2.5c}$$

and

$$g(t,t')=\tfrac{1}{2}|t-t'|+\tfrac{1}{2}(t+t')-\tfrac{1}{2}(t^2+t'^2)-\tfrac{1}{3}. \tag{2.5d}$$

The iteration of (2.5a) gives $P(t)$ for small Δ. To the first approximation, $P=\alpha\Delta^3P_0$ and

$$\kappa/\kappa_0=-2\alpha\Delta^3P_0(1)+O(\Delta^6). \tag{2.6}$$

For the Pippard kernel, $P_0(1)$ can be obtained in closed

[14] Herbert B. Dwight, *Tables of Integrals and Other Mathematical Data* (The Macmillan Company, New York, 1947), rev. ed., p. 182.

[15] F. Odeh, Internal report, IBM Research Center, Yorktown Heights, New York (unpublished).

form using iterates of the function $z(x)$ defined in ST, that is,

$$u(x)=-u(-x)=\int_0^x z(t)dt=\frac{x^2}{3}-\frac{x}{4}+\frac{2}{15}$$
$$-e^{-x}\left[\frac{2}{15}-\frac{7x}{60}+\frac{3x^2}{20}+\frac{x^3}{120}-\frac{x^4}{120}\right.$$
$$\left.-\left(\frac{x^3}{6}-\frac{x^5}{120}\right)E(x)\right],\quad (x\geq 0),\quad (2.7)$$

and

$$v(x)=v(-x)=\int_0^x u(t)dt=\frac{x^3}{9}-\frac{x^2}{8}+\frac{2x}{15}-\frac{1}{12}$$
$$-e^{-x}\left[-\frac{1}{12}+\frac{x}{20}-\frac{x^2}{30}+\frac{7x^3}{180}+\frac{x^4}{720}-\frac{x^5}{720}\right.$$
$$\left.-\left(\frac{x^4}{24}-\frac{x^6}{720}\right)E(x)\right],\quad (x\geq 0).\quad (2.8)$$

These functions are useful as well in the nonlocal-nonlinear considerations of Sec. 2 of the present paper.

To obtain the expression for $P_0(1)$, one can first integrate by parts twice in (2.4b), which gives

$$f(t)=\frac{1}{\Delta^2}f_1(s)=\frac{1}{\Delta^2}\int_0^\Delta k(|s-s'|)\left(s'-\frac{\Delta}{2}\right)ds'$$
$$=\frac{1}{2\Delta}[y(\Delta-s)-y(s)]$$
$$-\frac{1}{\Delta^2}[z(\Delta-s)-z(s)].\quad (2.9)$$

In terms of the variables s, s' the generalized Green's function becomes

$$G(s,s')=\tfrac{1}{2}|s-s'|+\tfrac{1}{2}(s+s')$$
$$-(2\Delta)^{-1}(s^2+s'^2)-\tfrac{1}{3}\Delta,\quad (2.10)$$

and

$$P_0(t)=\frac{1}{\Delta^4}\int_0^\Delta G(s,s')f_1(s')ds',\quad (2.11)$$

where

$$f_1(s)=\Delta^2 f(t)$$

as in (2.9). The integration in (2.11) can again be carried out by parts, using $\eta(s)=\int_0^s f_1(s')ds'$, $\zeta(s)=\int_0^s \eta(s')ds'$, and $\gamma(s)=\int_0^s \zeta(s')ds'$. One finds

$$P_0(t)=\frac{1}{\Delta^4}\left[G(s,\Delta)\eta(\Delta)-G(s,0)\eta(0)+\zeta(s)\right.$$
$$\left.-\frac{1}{\Delta}\gamma(\Delta)\right].\quad (2.12)$$

Furthermore,

$$\eta(s)=\tfrac{1}{2}\Delta[z(\Delta)-z(\Delta-s)-z(s)]$$
$$-[u(\Delta)-u(\Delta-s)-u(s)],\quad (2.13)$$

$$\zeta(s)=\tfrac{1}{2}\Delta[sz(\Delta)-u(\Delta)+u(\Delta-s)-u(s)]$$
$$-[su(\Delta)-v(\Delta)+v(\Delta-s)-v(s)],\quad (2.14)$$

$$\gamma(s)=\tfrac{1}{2}\Delta[\tfrac{1}{2}s^2z(\Delta)-su(\Delta)+v(\Delta)-v(\Delta-s)-v(s)]$$
$$-[\tfrac{1}{2}s^2u(\Delta)-sv(\Delta)+w(\Delta)$$
$$-w(\Delta-s)-w(s)].\quad (2.15)$$

The function $w(s)=\int_0^s v(s')ds'$ is not needed explicitly because in $\gamma(\Delta)$ the terms in w cancel.

Noticing that $\eta(0)=\eta(\Delta)=0$, (2.12) becomes

$$P_0(t)=(1/\Delta^4)[\zeta(s)-\Delta^{-1}\gamma(\Delta)],\quad (2.16)$$

and from (2.6), (2.14), (2.15), (2.16),

$$\kappa/\kappa_0=-2\alpha\left[\frac{1}{\Delta}v(\Delta)-u(\Delta)+\frac{\Delta}{4}z(\Delta)\right]+O(\Delta^6).\quad (2.17)$$

Finally, it can be verified directly that, for small x,

$$z(x)=\frac{x^2}{2}e^{-x}E(x)+\frac{x^2}{2}+o(x^2);$$
$$u(x)=\frac{x^3}{6}e^{-x}E(x)+\frac{2x^3}{9}+o(x^3);\quad (2.18)$$
$$v(x)=\frac{x^4}{24}e^{-x}E(x)+\frac{19x^4}{288}+o(x^4),$$

where $E(x)\sim-\ln x$. Thus, the leading term in κ/κ_0 is

$$(\kappa/\kappa_0)_{\text{Pippard}}\approx(\alpha/16)\Delta^3.\quad (2.19)$$

In the case of the BCS kernel, $k^*(u)$, one needs the asymptotic behavior for small u. At temperature $T=0$, $k^*(u)$ is defined by (1.1) and (1.2). According to (1.7), one has

$$I(r)=1+(4/\pi^2)r\ln r+O(r),\quad r\ll 1$$

and it is easy to see that

$$I(r)=O(e^{-r}),\quad r\gg 1.$$

One can write

$$k^*(s)=\int_s^\infty \frac{1}{r}I(r)dr-s^2\int_s^\infty \frac{1}{r^3}I(r)dr$$
$$=I_1(s)+I_2(s).$$

As $s\to 0$, $I_2(s)$ tends to a constant while, for fixed ϵ

$$I_1(s)=\int_s^\epsilon \frac{1}{r}I(r)dr+\int_\epsilon^\infty \frac{1}{r}I(r)dr$$
$$=\int_s^\epsilon \frac{1}{r}\left[1+\frac{4}{\pi^2}r\ln r\right]dr+\int_s^\epsilon \frac{O(r)}{r}dr$$
$$+\int_\epsilon^\infty O\left(\frac{e^{-r}}{r}\right)dr.\quad (2.20)$$

The asymptotic behavior of $I_1(s)$ for $s\to 0$ is thus dominated by the contributions from the lower limit of the first term on the right side of (2.20). Hence,

$$k^*(s)\sim -\ln|s|-(4/\pi^2)|s|\ln|s|+O(1)+O(s)+\cdots.$$

The corresponding expression in the Pippard case is $k(s)\sim -\ln|s|$. One finds then easily that

$$f^*(t)=f(t)-(4/\pi^2)\Delta\ln\Delta q(t)+O(\Delta),$$

where $f^*(t)$ is the BCS analog of $f(t)$ defined by (2.4b) and $q(t)=(t^2/2)-t^3+(7/12)$. Substitution in (2.5b) gives

$$P_0^*(1)=P_0(1)-(4/51\pi^2)\Delta\ln\Delta+O(\Delta). \quad (2.21)$$

The second term in (2.21) is due to the logarithmic term in the BCS kernel and is responsible for the slightly lower susceptibilities in the BCS model in the thin-film limit. Using (2.6), (2.19), and (2.21), the expression for the latter becomes

$$\kappa/\kappa_0^*=\tfrac{1}{16}\alpha\Delta^3+(8/51\pi^2)\alpha\Delta^4\ln\Delta+\cdots. \quad (2.22)$$

B. Critical and Maximum Fields

(i) *The Weak Field Model*

London[16] gave a method of calculating critical fields by equating the energy density in the normal state to that in the superstate, calculated from the London theory. Here, the critical field is calculated on the same basis except that the nonlocal relations are employed.

Let

$$J(x)=-\frac{c}{4\pi}\int K(x-\xi)A(\xi)d\xi \quad (2.23)$$

be true for all time. Then, by differentiating and using Maxwell's equations, one gets

$$E(x,t)=\int R(x,\xi)\frac{\partial}{\partial t}J_s(\xi,t)d\xi, \quad (2.24)$$

where R is a kernel which can be obtained from K. In fact, in a bulk material $R(x,\xi)=R(|x-\xi|)$ and $R(t)=(c^2/4\pi)\mathfrak{F}^{-1}[(\mathfrak{F}K(t))^{-1}]$ where $\mathfrak{F}$ denotes the operation of taking the Fourier transform. It can be proved, along the lines of London's theory, that, if (2.24) holds and if surface energies are neglected, the total energy G_s in a superconducting film of thickness D in the static case, is equal to

$$G_s=\frac{1}{8\pi}\int_0^D H_s^2dx+\frac{1}{2}\int_0^D\int_0^D R(x,\xi)J(x)J(\xi)dxd\xi.$$

In equilibrium, the normal and super energies are equal and one gets, for determining the critical field, H_c, the equation

$$\frac{D}{8\pi}H_c^2=\frac{D}{8\pi}H_{cb}^2+\frac{1}{8\pi}\int_0^D H_s^2dx+\frac{1}{2}\int_0^D\int_0^D R(x,\xi)J(x)J(\xi)dxd\xi, \quad (2.25)$$

where H_{cb} is the bulk critical field.

Instead of using (2.24), one may assume that the electric field is governed by London's second local relation $(\partial/\partial t)(\Lambda J)=E$. In this case, (2.25) simplifies to

$$DH_c^2=DH_{cb}^2+\int_0^D\{H_s^2+4\pi\Lambda J^2(x)\}dx. \quad (2.26)$$

In terms of the dimensionless field potential, F, defined in ST, (2.26) becomes

$$\left(\frac{H_c}{H_{cb}}\right)^2=\left\{1-\frac{1}{\Delta}\int_0^\Delta\left[\left(\frac{dF}{ds}\right)^2+\frac{\lambda_0^2}{\xi^2}\left(\frac{d^2F}{ds^2}\right)^2\right]ds\right\}^{-1}. \quad (2.27)$$

The use of the nonlocal relation (2.25) gives rise to a higher critical field than the one defined by (2.27).

In (2.27) the values $F'(s_i)$ and $F''(s_i)$ can be obtained by numerically differentiating the $F(s_i)$ values, calculated according to Sec. 1 on the grid $\{s_i\}$, using symmetrical or unsymmetrical three point differentiation formulas[17] at the interior and extreme grid points, respectively. The integral is then evaluated by Simpson's rule.

(ii) *The Strong Field Model*

In order to take the strong field effects, as well as nonlocal effects, into account, Bardeen's generalization[1] of the GL equations has been used. To simplify matters, let $\xi=\xi_0$ in this subsection. Consider again a plane film of width D in a uniform parallel magnetic field, H_e. The Bardeen equations for the vector potential $\mathfrak{A}(x)$ and order parameter $\psi(x)$ read

$$\frac{d^2\psi}{dx^2}=\frac{2m}{\hbar^2}\beta\psi^3-\frac{2m}{\hbar^2}|\alpha|\psi+\frac{e^2}{\hbar^2c^2}\mathfrak{A}(x)\int_0^D K(|x-x'|)\psi(x')\mathfrak{A}(x')dx', \quad (2.28)$$

$$\frac{d^2\mathfrak{A}}{dx^2}=\frac{4\pi e^2}{mc^2}\psi(x)\int_0^D K(|x-x'|)\psi(x')\mathfrak{A}(x')dx', \quad (2.29)$$

where the constants and the kernel K are defined as in Bardeen[1] and the integrations on the right side of (2.28), (2.29) are over the film only because diffuse

[16] Fritz London, *Superfluids, Macroscopic Theory of Superconductivity* (Dover Publications, Inc., New York, 1960), 2nd ed., Vol. 1, p. 131.

[17] William E. Milne, *Numerical Calculus* (Princeton University Press, Princeton, New Jersey, 1949), p. 96.

scattering on the boundary will be assumed. Introduce now the nondimensional quantities $z=x/\lambda_0$, $d=D/\lambda_0$, where λ_0 is the weak-field penetration depth. Define the normalized order parameter, $\phi(z)$, vector potential, $A^{(1)}(z)$, and kernel $k^{(1)}(z)$ by

$$\phi(z)=\frac{\psi(x)}{\psi_\infty(x)}=\frac{\psi(x)}{(|\alpha|/\beta)^{1/2}},$$

$$A^{(1)}(z)=\frac{\mathfrak{A}(x)}{\sqrt{2}H_{cb}\lambda_0}=\left(\frac{e^2}{2mc^2|\alpha|}\right)^{1/2}\mathfrak{A}(x),$$

$$k^{(1)}(z)=\tfrac{4}{3}\xi K(|x|),$$

where H_{cb} is the bulk critical field, and the superscript indicates that the present normalization is different from the one used in Sec. 1. In terms of these variables, and the nonlinear coupling constant $\kappa^2=(\beta/2\pi)(mc/e\hbar)^2$, Eqs. (2.28), (2.29) reduce to

$$\frac{d^2A^{(1)}(z)}{dz^2}=\tfrac{3}{4}\phi(z)\left(\frac{\lambda_0}{\xi}\right)\int_0^d k^{(1)}(|z-z'|)\times\phi(z')A^{(1)}(z')dz', \quad (2.30)$$

$$\frac{d^2\phi(z)}{dz^2}=\kappa^2\left[\phi^3(z)-\phi(z)+\tfrac{3}{4}A^{(1)}(z)\left(\frac{\lambda_0}{\xi}\right)\times\int_0^d k^{(1)}(|z-z'|)\phi(z')A^{(1)}(z')dz'\right]. \quad (2.31)$$

The kernel $k^{(1)}(z)$ is given by

$$k^{(1)}(|z|)=\int_1^\infty\left(\frac{1}{t}-\frac{1}{t^3}\right)\exp[-(\lambda_0/\xi)|z|t]dt,$$

for the Pippard case,

$$=\int_1^\infty\left(\frac{1}{t}-\frac{1}{t^3}\right)J(|z|\lambda_0 t,\xi_0)dt,$$

for the BCS case at $T=0$.

The boundary conditions imposed on $\phi(z)$ and $A^{(1)}(z)$ are, as usual,

$$\left.\frac{d\phi(z)}{dz}\right|_{0,d}=0, \quad (2.32)$$

$$\left.\frac{dA^{(1)}(z)}{dz}\right|_{0,d}=h_e=\frac{H_e}{\sqrt{2}H_{cb}}, \quad (2.33)$$

where H_e is the applied magnetic field.

Equations (2.30), (2.31) may be solved for small κ^2, or small d, as follows. Expand $\phi(z)$ and $A^{(1)}(z)$ in power series of κ^2,

$$\phi(z,\kappa^2)=\sum\kappa^{2n}\phi_n(z),$$

$$A^{(1)}(z,\kappa^2)=\sum\kappa^{2n}A_n{}^{(1)}(z).$$

Substituting in (2.31), the boundary conditions (2.32) imply that $\phi_0(z)$ is some constant, ϕ. Equation (2.30), with the boundary conditions (2.33), may now be solved for $A_0{}^{(1)}(z)$ with ϕ as a parameter. The solvability condition for $\phi_1(z)$ then implies that the integral of the right side of (2.31), with ϕ and $A_0{}^{(1)}(z)$ substituted for $\phi(z)$ and $A^{(1)}(z)$, respectively, must vanish. This gives a relationship between ϕ and h_e which reads

$$d(\phi^2-1)+\frac{3}{4}\left(\frac{\lambda_0}{\xi}\right)h_e{}^2\int_0^d F^{(1)}(z)\times\int_0^d k^{(1)}(|z-z'|)F^{(1)}(z')dz'dz=0, \quad (2.34)$$

where $F^{(1)}$ is the solution of (2.30), with $\phi(z)=\phi$ and $dF^{(1)}/dz|_{0,d}=1$.

Following Marcus,[10] the relation (2.34) may be called the "equation of state" of the film. Restricting ϕ to the interval (0,1), one finds that (2.34) imposes an upper bound on h_e such that $h_e\leq h_m$. It is this maximum field, h_m, that has been referred to by Douglass,[18] in his discussion of the GL equations, as the critical field. As pointed out by Marcus, h_m is actually the superheating field, while the transition field, h_c, is defined by the first intersection of the curves of the equation of state and the relationship $G_s=G_n$ where G_s, G_n are the Gibbs free-energy densities in the super and normal states. In this report, only the maximum field, h_m, will be considered (see next section).

The equation of state (2.34) can be brought into the form

$$\Delta(\phi^2-1)+\frac{3\xi_0{}^2}{4\lambda_0{}^2}h_e{}^2\int_0^\Delta F(s)\int_0^\Delta k(|s-s'|)\times F(s')ds'ds=0, \quad (2.35)$$

where the notations of Sec. 1 are used and $F(s)$ is the solution of the basic equation (2.6) of ST *with a new definition of* α:

$$\alpha=3\xi_0{}^2\phi^2/4\lambda_0{}^2. \quad (2.36)$$

The equations of state can thus be computed, using the numerical field distributions obtained according to Sec. 1, by numerically evaluating the double integral in (2.35). In practice, the trapezoidal rule has been used.

As in the calculation of susceptibilities there is, however, an extreme case in which an analytical treatment is not only possible but gives more accurate results than the numerical methods. This is the case when ϕ^2 is small. Recalling the definition $\Delta=D/\xi$ and assumption $\xi=\xi_0$, it follows from (2.35) that

$$h_e{}^2=\frac{4\Delta^3\lambda_0{}^2}{3D^2}(1-\phi^2)\Big/Y, \quad (2.37)$$

[18] D. H. Douglass, Phys. Rev. **124**, 735 (1961).

with

$$Y=\int_0^\Delta F(s)\int_0^\Delta k(|s-s'|)F(s')ds'ds. \quad (2.38)$$

For small ϕ^2 one can write

$$F(s)=F_0(s)+\phi^2F_1(s)+\cdots,$$

and

$$Y=Y_0+\phi^2Y_1+\cdots.$$

By the techniques used in the discussion of susceptibilities, one finds

$$F(s)=(s-\tfrac{1}{2}\Delta)+P_1(s),$$
$$P_1(s)=P_{1,0}(s)+O(\alpha^2),$$
$$P_{1,0}(s)=\alpha\int_0^\Delta G(s,s')f_1(s')ds',$$

where f_1 and G are defined by (2.9) and (2.10), respectively. Furthermore,

$$Y_0=\int_0^\Delta (s-\tfrac{1}{2}\Delta)f_1(s)ds,$$
$$Y_1=\frac{3\xi_0^2}{2\lambda_0^2}\int_0^\Delta\int_0^\Delta G(s,s')f_1(s)f_1(s')dsds'. \quad (2.39)$$

In terms of the auxiliary functions $z(s)$, $u(s)$, and $v(s)$ introduced above, one finds

$$Y_0=-\tfrac{1}{2}\Delta^2z(\Delta)+2\Delta u(\Delta)-2v(\Delta), \quad (2.40)$$

while Y_1 can be calculated by numerical quadrature. Writing

$$h_e=h_{e,0}+\phi^2h_{e,1}+\cdots, \quad (2.41)$$

one obtains

$$h_{e,0}=\frac{2}{\sqrt{3}(D/\lambda_0)}\times\frac{1}{(Y_0/\Delta^3)^{1/2}}=h_e(0). \quad (2.42)$$

This result is important independently of whether the equation of state is studied for small ϕ^2 only or not, as will be seen in the discussion of the results in Sec. 3.

It is particularly interesting to consider two special cases:

(a) the case $\Delta\to\infty$, that is, the bulk case ($D\to\infty$ or $\xi=\xi_0\to 0$). If one neglects terms $O(e^{-\Delta})$ versus negative powers of Δ, one finds

$$h_{e,0}\approx\frac{2\sqrt{3}}{D/\lambda_0}\left(1-\frac{9}{8\Delta}+\frac{3}{2\Delta^3}\right)^{-1/2}. \quad (2.43)$$

Furthermore,

$$h_{e,1}=-\tfrac{1}{2}h_{e,0}\left(1+\frac{Y_1\Delta^{-3}}{Y_0\Delta^{-3}}\right), \quad (2.44)$$

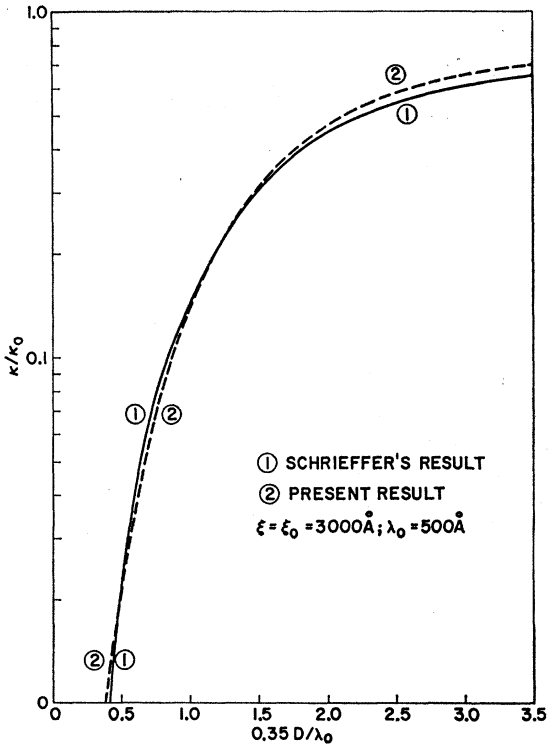

FIG. 1. Susceptibilities. Comparison with Schrieffer's variational results.

and the numerical results indicate that

$$Y_1\Delta^{-3}=(D/\lambda_0)^2\theta(\Delta) \quad (2.45)$$

tends to a limit when $\Delta\to\infty$, just as $Y_0\Delta^{-3}$ does;

(b) the case $\Delta\to 0$, that is, the thin-film limit. From (2.17), (2.19), (2.40), (2.42) it follows that, in this limit,

$$h_e(0)=(\kappa/\kappa_0)^{-1/2}\approx 4/(\alpha\Delta^3)^{1/2}$$
$$=(8/\sqrt{3})(\xi_0\lambda_0^2/D^3)^{1/2}. \quad (2.46)$$

3. SUMMARY OF THE RESULTS

A. Susceptibilities and Magnetic-Field Distributions

The solution to the nonlocal equations clearly depends on two parameters only, namely $\Delta=D/\xi$ and $\alpha=3\xi^3/4\xi_0\lambda_0^2$, and, of course, on the form of the normalized kernel. Hence, the susceptibilities and the magnetic-field distributions in plane films depend on these parameters only. This is the same situation as in the specular reflection case. The main results of the present investigation are the following:

(1) A comparison between the susceptibilities calculated from Schrieffer's[3] solution in the diffuse scattering case and the present solution is made in Fig. 1. The present values are higher then Schrieffer's susceptibilities for relatively thick and very thin films. The difference is about 20% at a thickness of one penetration

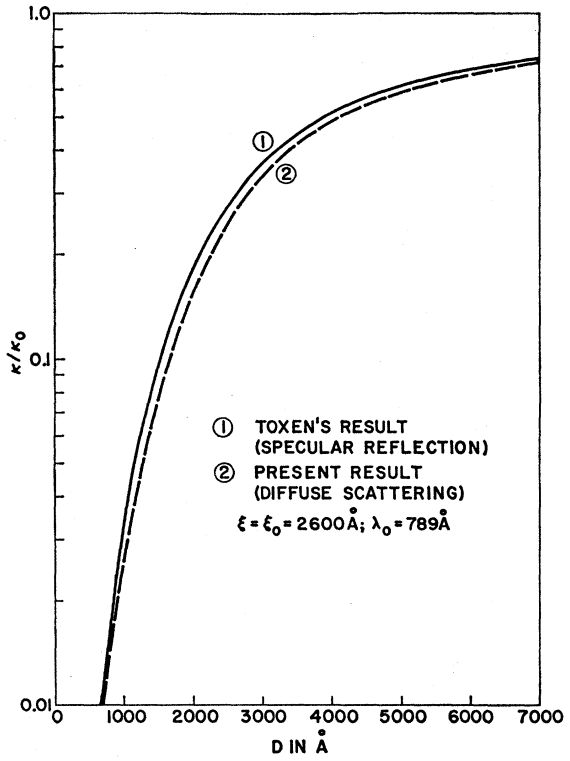

FIG. 2. Susceptibilities. Comparison with Toxen's results for specular reflection.

depth and 7% at 10 penetration depths. A lower susceptibility (about 10%) is found at intermediate thicknesses of two to three penetration depths. (Because of the wide range of variation of κ/κ_0, semilogarithmic representation is used which tends to make the agreement look better than it is.)

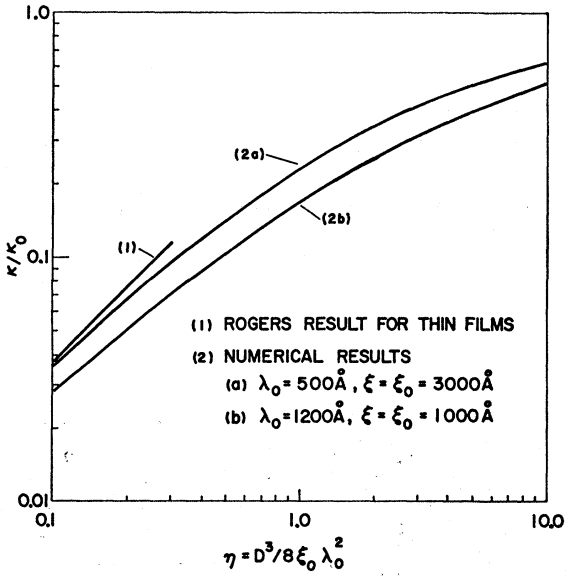

FIG. 3. Variation of the susceptibilities with coherence length and penetration depth for fixed "natural" parameter of Rogers.

(2) Figure 2 gives a comparison of susceptibilities, using the Pippard kernel, for the cases of diffuse and specular reflection. The latter case was calculated by Toxen.[6] The diffuse boundary condition always gives a lower susceptibility. For example, the difference is about 20% for $D/\lambda_0=2$. As expected, the diffuse and specular reflection results approach each other for both the thin-film and bulk-material limits. For bulk materials, however, this approach is rather slow (see Fig. 2).

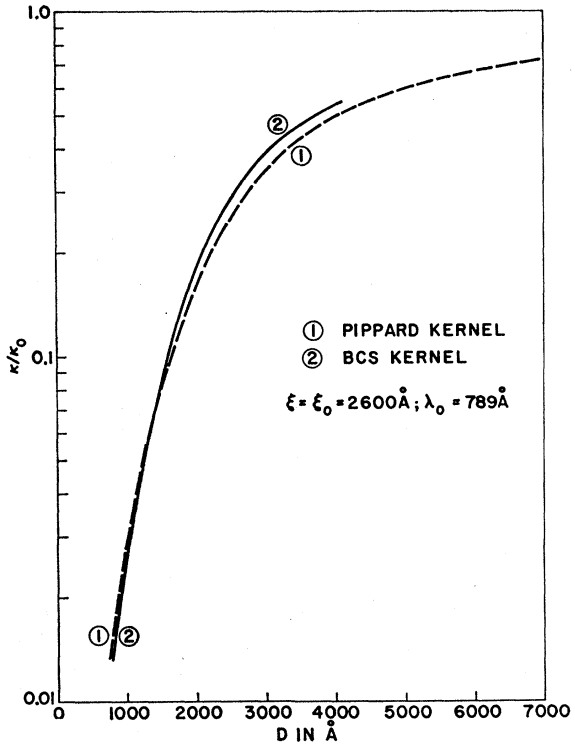

FIG. 4. Susceptibilities. Comparison between Pippard and BCS kernels.

(3) Figure 3 emphasizes the fact that two parameters are always needed to describe the nonlocal effect. Rogers[8] plotted the susceptibility against the "natural parameter of nonlocal models," namely, $\eta=D^3/8\xi_0\lambda_0^2$. In Fig. 3, the susceptibility is represented as a function of η with $\xi=\xi_0$, and it is shown that, be changing the nonlocal parameters, keeping η fixed, quite different results may be obtained. For example, a 40% higher susceptibility may be obtained by reducing λ_0 from 1200 to 500 Å and increasing ξ from 1000 to 3000 Å, with a fixed value $\eta=0.5$.

(4) In the thin-film limit, the method used in Sec. 2 gives, for the susceptibility in the Pippard case, relation (2.19). This result is equivalent to the one of Rogers[8] which was calculated from Schrieffer's variational solution. Curve 1 in Fig. 3 represents this result (whereas, apparently, curve (c) in Fig. 1B of Rogers[8]

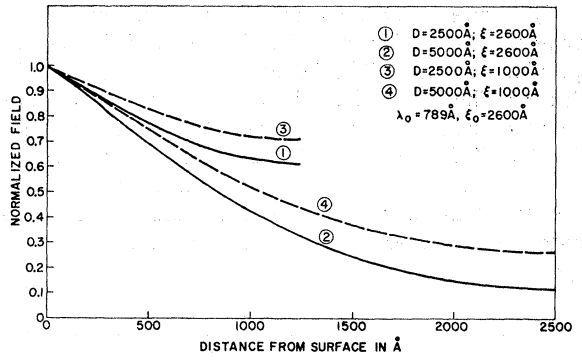

FIG. 5. Field distributions. Dependence on coherence length and thickness.

does not). In the specular reflection case, the value calculated by Toxen[6] is $\kappa/\kappa_0=(0.0824)\alpha\Delta^3+O(\Delta^4)$.

(5) The results of the calculation with the BCS kernel are qualitatively similar to the Pippard case. One may note, however:

(a) The susceptibility calculated with the BCS kernel is slightly lower than that with the Pippard kernel for thin films, but becomes higher for relatively thick ones (Fig. 4) and apparently converges to the Pippard susceptibility for bulk materials. This may be traced back to the fact that the areas under the truncated BCS and Pippard kernels exhibit a corresponding behavior.

(b) In the thin film approximation, the susceptibility is no longer a simple power series of thickness. In fact, because of the behavior of $I(r)$ near zero, as the equation following (2.19) shows, logarithmic terms appear. The second term on the right side of (2.22) is negative for small Δ and is responsible for the lower susceptibilities in the BCS model. For example, taking $\Delta=0.1$, one finds a difference of approximately 6% between the two models.

(6) In Figs. 5 and 6, typical field distributions are plotted. Only half the film is shown in each case. In Fig. 5 one notices that, for fixed D and ξ_0, the field decreases with increasing coherence length ξ so that for a large coherence length, it may be anticipated that the magnetic field will reverse its sign. This sign reversal has been observed in the calculations. If ξ and ξ_0 are fixed, then again an increasing thickness causes a decrease and, eventually, the sign reversal of the magnetic field. In Fig. 6, a comparison between the field distributions in the Pippard and BCS models is shown. For the thicknesses used—which range from 1.5 to 3 penetration depths—the BCS model gives a lower magnetic field. However, the opposite should be true in the thin-film limit.

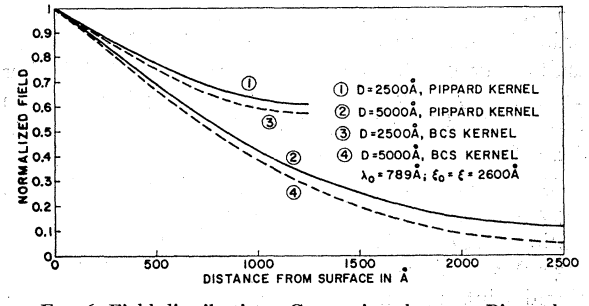

FIG. 6. Field distributions. Comparison between Pippard and BCS kernels.

B. Critical and Maximum Fields

(1) *The Nonlocal Weak Field Model*

The London-type calculation of Sec. 2 leads to expression (2.27) for the normalized critical field $H=H_c/H_{cb}$. Figure 7 shows a plot of H as a function of half-thickness, for some fixed nonlocal parameters. When compared with the results of Toxen,[6] the plot shows that the nonlocal weak field calculation overestimates the critical field of thin films while the London theory underestimates it. Figure 8 shows that, in either model, the critical field decreases with increasing coherence length but increases when the penetration depth does.

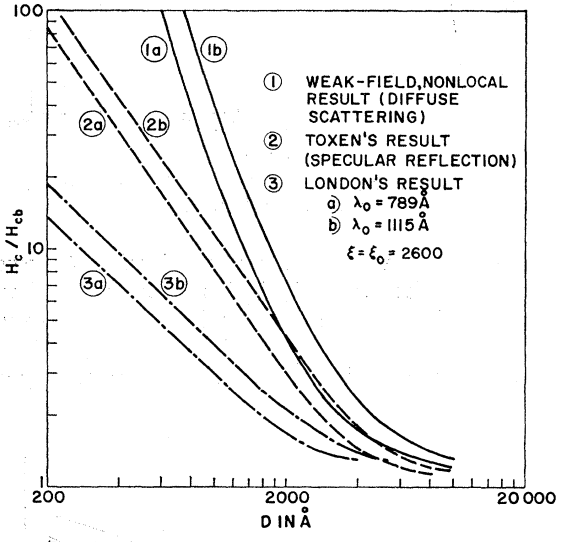

FIG. 7. Critical fields. Nonlocal weak field model. Comparison with Toxen's and London's results.

(2) *The Strong Field Model*

(*a*) *Equation of state.* In Figs. 9, 10, and 11, equations of state, defined by (2.35) and computed with the Pippard kernel, are represented for $\xi=\xi_0$ and various values of D, ξ, and λ_0. One finds that the field h_e, corresponding to a certain value of the order parameter, increases, for fixed D/λ_0, as ξ/D increases, but decreases for fixed ξ/D and increasing D/λ_0. For example, $h_e(0)$ for $\xi/D=2$ is roughly twice as big as $h_e(0)$ for $\xi/D=0$.

The limiting curves for $\xi/D=0$ have been calculated analytically by Marcus [10] and copied here for the sake of comparison with the results of the nonlocal-nonlinear theory. It appears that, as $\xi/D\to 0$, the equation of state (2.35) goes over smoothly into the one for the Ginzburg-Landau theory given by Marcus. As far as the value h_e ($\phi=0$) is concerned, this can be shown analytically by letting $\Delta\to\infty$ in (2.43). The numerical results, including a direct computation of $d^2h_e/d\phi^2$ at $\phi=0$, indicate the same behavior.

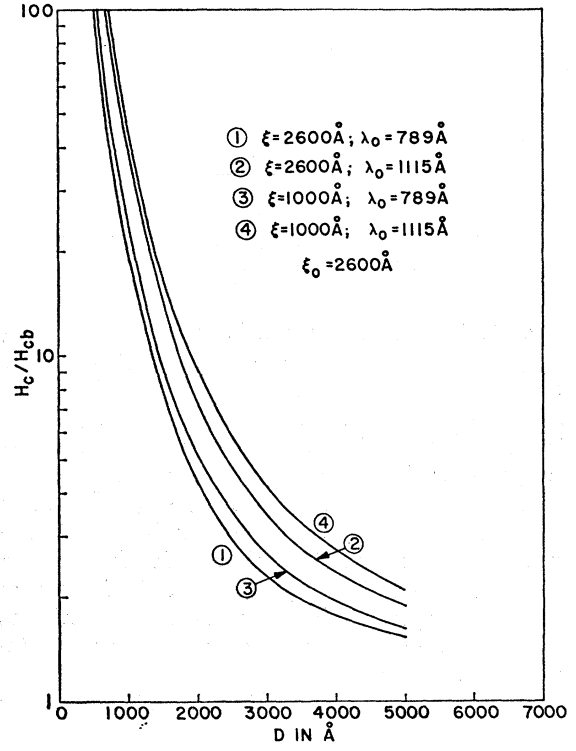

FIG. 8. Critical fields. Nonlocal weak field model. Dependence on thickness, coherence length, and penetration depth.

(*b*) *Type of transition.* In the GL case, one distinguishes two types of transitions. Depending on whether $h_e(\phi)$ takes its maximum, h_m, at a value of $\phi>0$ or at $\phi=0$, the transition is first or second order. Marcus's solution for the GL case gives, for small ϕ,

$$h_e\approx[2\sqrt{3}/(D/\lambda_0)]\{1-\tfrac{1}{2}[1-(D/\lambda_0)^2/5]\phi^2+O(\phi^4)\}.$$

The transition is thus first or second order depending on whether $D/\lambda_0>\sqrt{5}$ or $D/\lambda_0<\sqrt{5}$, respectively.

Combining (2.41), (2.44), and (2.45), one finds that, for $\xi/D\neq 0$, this state of affairs is preserved, at least for not too large values of ξ/D. One obtains

$$h_e(\phi,\Delta)=h_e(0,\Delta)\left\{1-\frac{1}{2}\left[1+\frac{(D/\lambda_0)^2\theta(\Delta)}{Y_0\Delta^{-3}}\right]\phi^2+O(\phi^4)\right\},$$

so that the transition is first or second order depending

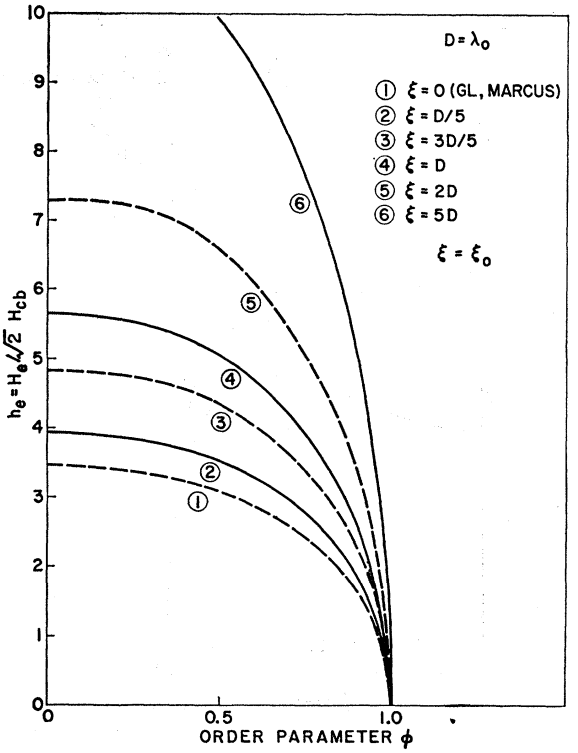

FIG. 9. Nonlocal-nonlinear model. Equations of state. I.

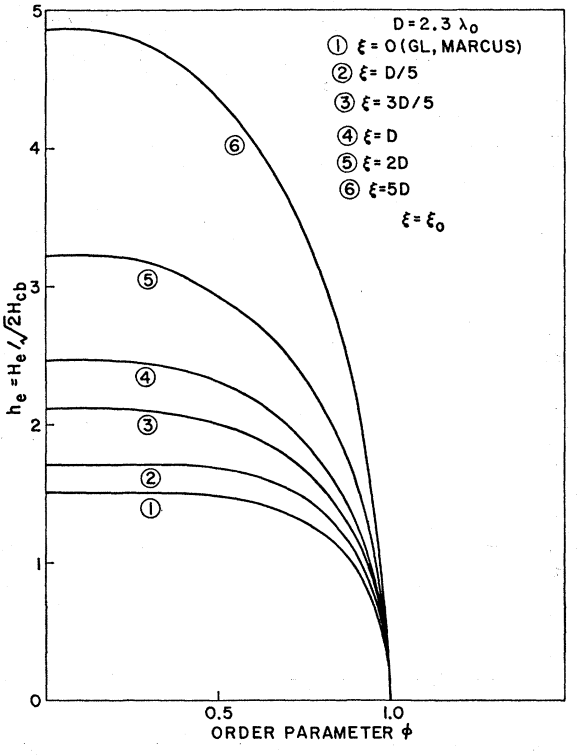

FIG. 10. Nonlocal-nonlinear model. Equations of state. II.

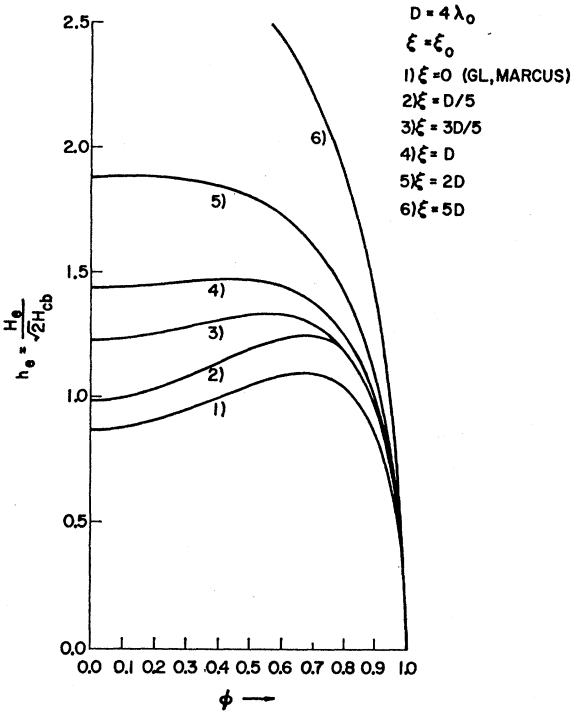

FIG. 11. Nonlocal-nonlinear model. Equations of state. III.

on whether $D/\lambda_0 > (D/\lambda_0)_{\text{crit}}$ or $D/\lambda_0 < (D/\lambda_0)_{\text{crit}}$, where

$$(D/\lambda_0)_{\text{crit}} = [-(Y_0/\Delta^3)/\theta(\Delta)]^{1/2}.$$

According to (2.42) and (2.43), $\lim_{\Delta\to\infty}(Y_0\Delta^{-3}) = \frac{1}{9}$. The numerical results indicate that $\lim_{\Delta\to\infty}\theta(\Delta) = -1/45$, so that $\lim_{\Delta\to\infty}(D/\lambda_0)_{\text{crit}} = \sqrt{5}$, the critical value for the GL case. $(D/\lambda_0)_{\text{crit}}$ increases with ξ as Fig. 12 shows. This means that, for a given $D/\lambda_0 > \sqrt{5}$, the type of transition can be changed from first order to second order by raising ξ sufficiently for $(D/\lambda_0)_{\text{crit}}$ to exceed the given D/λ_0. This situation is represented

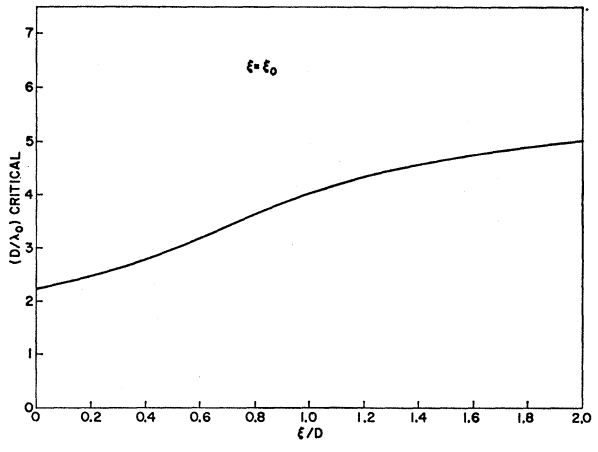

FIG. 12. Nonlocal-nonlinear model. Dependence of critical thickness on coherence length.

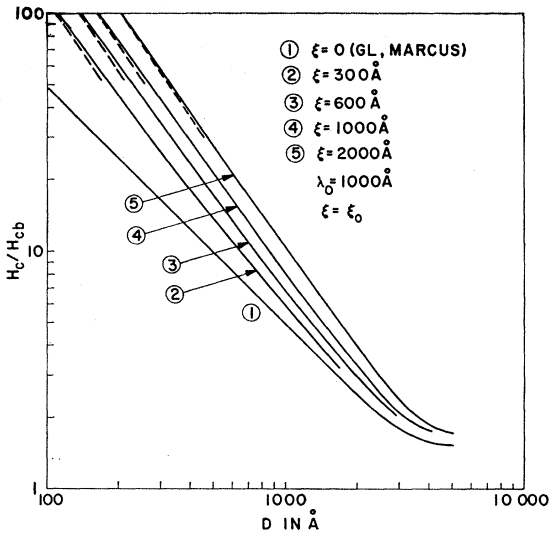

FIG. 13. Nonlocal-nonlinear model. Dependence of maximum field on thickness and coherence length.

in Fig. 11. On the other hand, for sufficiently small ξ, the type of transition is the same as for $\xi = 0$. This is obvious for $D/\lambda_0 \neq \sqrt{5}$. For $D/\lambda_0 = \sqrt{5}$, it follows from the fact that the transition is second order at $\xi = 0$.

As pointed out in Sec. 2, maximum fields have been investigated as functions of thickness and coherence length. The results, $H_m/H_{cb} = (H_e/H_{cb})_{\max} = \sqrt{2}h_m$ based on the Pippard kernel, are represented in Fig. 13. The lowest curve represents Marcus' result for the GL case. For $\xi/D > 0$ and $D/\lambda_0 < (D/\lambda_0)_{\text{crit}}$, that is, for second order transition, $h_m = h_e(\phi = 0)$ is given analytically by (2.40), (2.42). As there is no superheating when the transition is second order, it appears that $h_c = h_m$ in this case. In this sense, in the thin-film limit, the present

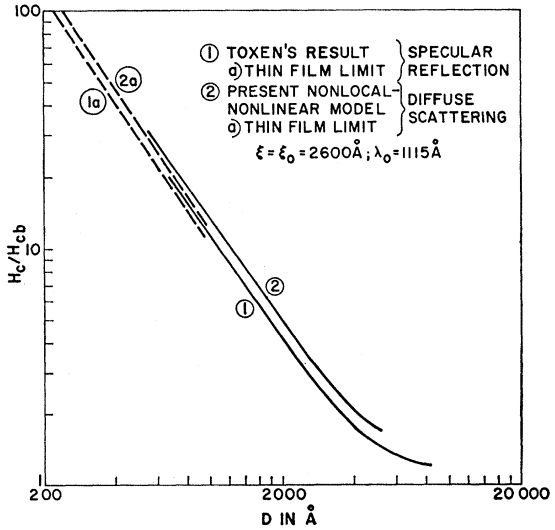

FIG. 14. Nonlocal-nonlinear model. Maximum field. Comparison with Toxen's critical fields for specular reflection.

nonlocal-nonlinear considerations rigorously prove the $D^{-3/2}$ dependence of the critical field according to (2.46). This result [that is, $H_c/H_{cb}=\sqrt{2}h_e(0)$] is represented by the asymptotes in the upper left-hand part of Fig. 13. For $D/\lambda_0>(D/\lambda_0)_{\text{crit}}$, that is, for first order transition, the maximum fields have been determined numerically between discrete points of the equation of state. Figure 13 shows that, for fixed ξ and λ_0, the maximum field decreases with increasing thickness, but for fixed D and λ_0, the maximum field increases with ξ.

(*c*) *Comparison with Toxen's critical fields.* The maximum fields calculated by the methods of the present paper have been compared with Toxen's critical fields which were obtained from a different model.[6] In the thin-film limit, the present result (2.46) and Toxen's result for random scattering are equivalent. In Fig. 14, this result is represented by the asymptote (2a). In the general case (that is, for thicker films) the present maximum fields for diffuse scattering (curve 2) are higher than Toxen's critical fields for specular reflection (curves 1, 1a), but, qualitatively, they show the same behavior.

ACKNOWLEDGMENT

The authors would like to thank H. Cohen, A. M. Toxen, P. M. Marcus, and W. R. Heller for many valuable suggestions and interesting discussions.

PHYSICAL REVIEW VOLUME 132, NUMBER 5 1 DECEMBER 1963

Low-Field de Haas–van Alphen Studies of Chromium Group Transition Elements

G. B. BRANDT AND J. A. RAYNE
Westinghouse Research Laboratories, Pittsburgh, Pennsylvania
(Received 29 July 1963)

De Haas–van Alphen measurements up to fields of 18 kG have been made on the chromium group of transition elements. The results indicate that only in the case of molybdenum do the relevant parts of the Fermi surface agree well with the Lomer model. For chromium the disagreement is very marked and results presumably from its antiferromagnetic ordering at low temperatures. Possible reasons for the behavior of tungsten are discussed.

I. INTRODUCTION

THE band structure of the chromium group of transition metals is of great experimental and theoretical interest. In the case of tungsten and molybdenum, magnetoresistance[1] and anomalous skin effect measurements[2] have shown that the Fermi surface of each metal is essentially compensated in character. The effective area of the Fermi surface is, moreover, less than that corresponding to a sphere containing one electron per atom, so that the free electron model is certainly not applicable to these metals.

Lomer[3] has recently advanced a model which is consistent with these results. Essentially, the proposed model postulates the existence of star-shaped electron and hole surfaces, situated at the zone center and zone corners, respectively. These surfaces, which contain roughly equal numbers of carriers, are degenerate along ⟨100⟩. Additional hole pockets are present at the centers of the zone faces, while along the cube axes are further small groups of electrons or holes. A similar band structure is predicted for nonmagnetic chromium. Lomer has considered the effects of antiferromagnetic ordering in the latter, but it is not clear what detailed modifications this would cause in the associated Fermi surface.

Recent dHvA[4] and magnetoacoustic[5] measurements have shown that, in the case of tungsten, the major parts of the Fermi surface are in essential agreement with the above model. This conclusion does not, however, apply to the small pockets of carriers along ⟨100⟩, neither set of data giving very complete information in this regard. Since the existence of these pockets is an essential feature of the model, detailed measurements of the low-field dHvA effect in tungsten are needed to investigate their presence and nature. In addition, a comparison with the dHvA effect in molybdenum and chromium is necessary to establish the consequences of antiferromagnetic ordering in the latter. For these reasons the present study[6] was undertaken.

The results indicate that only in molybdenum does the Lomer model provide an adequate description of the relevant part of the Fermi surface. In the case of tungsten additional periods are observed, one set of which are attributable to extremal orbits around the necks of the main electron surface. The remaining periods are

[1] E. Fawcett, Phys. Rev. **128**, 154 (1962).
[2] E. Fawcett and D. Griffiths, J. Phys. Chem. Solids **23**, 1631 (1962).
[3] W. M. Lomer, Proc. Phys. Soc. (London) **80**, 489 (1962).
[4] R. F. Girvan and A. V. Gold (private communication).
[5] J. A. Rayne and H. Sell, Phys. Rev. Letters **8**, 199 (1962).
[6] Preliminary results have already been reported: G. B. Brandt and J. A. Rayne, Phys. Letters **3**, 148 (1962); see also D. Sparlin and J. A. Marcus, Bull. Am. Phys. Soc. **8**, 258 (1963).